BIOCHEMISTRY
including biophysical chemistry & molecular biology

Article

pubs.acs.org/biochemistry

Investigating the Kinetic Mechanism of Inhibition of Elongation Factor 2 Kinase by NH125: Evidence of a Common in Vitro Artifact

Ashwini K. Devkota,[†] Clint D. J. Tavares,[†] Mangalika Warthaka,[‡] Olga Abramczyk,[‡] Kyle D. Marshall,[‡] Tamer S. Kaoud,[‡,§] Kivanc Gorgulu,[∥] Bulent Ozpolat,*[,∥] and Kevin N. Dalby*[,†,‡,§]

[†]Graduate Program in Cell and Molecular Biology, The University of Texas, Austin, Texas 78712, United States

[‡]Division of Medicinal Chemistry, College of Pharmacy, The University of Texas, Austin, Texas 78712, United States

[§]Graduate Program in Pharmacy, The University of Texas, Austin, Texas 78712, United States

[∥]Department of Experimental Therapeutics, University of Texas M. D. Anderson Cancer Center, Houston, Texas 77030, United States

Supporting Information

ABSTRACT: Evidence that elongation factor 2 kinase (eEF-2K) has potential as a target for anticancer therapy and possibly for the treatment of depression is emerging. Here the steady-state kinetic mechanism of eEF-2K is presented using a peptide substrate and is shown to conform to an ordered sequential mechanism with ATP binding first. Substrate inhibition by the peptide was observed and revealed to be competitive with ATP, explaining the observed ordered mechanism. Several small molecules are reported to inhibit eEF-2K activity with the most notable being the histidine kinase inhibitor NH125, which has been used in a number of studies to characterize eEF-2K activity in cells. While NH125 was previously reported to inhibit eEF-2K in vitro with an IC_{50} of 60 nM, its mechanism of action was not established. Using the same kinetic assay, the ability of an authentic sample of NH125 to inhibit eEF-2K was assessed over a range of substrate and inhibitor concentrations. A typical dose−response curve for the inhibition of eEF-2K by NH125 is best fit to an IC_{50} of 18 ± 0.25 μM and a Hill coefficient of 3.7 ± 0.14, suggesting that NH125 is a weak inhibitor of eEF-2K under the experimental conditions of a standard in vitro kinase assay. To test the possibility that NH125 is a potent inhibitor of eEF2 phosphorylation, we assessed its ability to inhibit the phosphorylation of eEF2. Under standard kinase assay conditions, NH125 exhibits a similar weak ability to inhibit the phosphorylation of eEF2 by eEF-2K. Notably, the activity of NH125 is severely abrogated by the addition of 0.1% Triton to the kinase assay through a process that can be reversed upon dilution. These studies suggest that NH125 is a nonspecific colloidal aggregator in vitro, a notion further supported by the observation that NH125 inhibits other protein kinases, such as ERK2 and TRPM7 in a manner similar to that of eEF-2K. As NH125 is reported to inhibit eEF-2K in a cellular environment, its ability to inhibit eEF2 phosphorylation was assessed in MDA-MB-231 breast cancer, A549 lung cancer, and HEK-293T cell lines using a Western blot approach. No sign of a decrease in the level of eEF2 phosphorylation was observed up to 12 h following addition of NH125 to the media. Furthermore, contrary to the previously reported literatures, NH125 induced the phosphorylation of eEF-2.

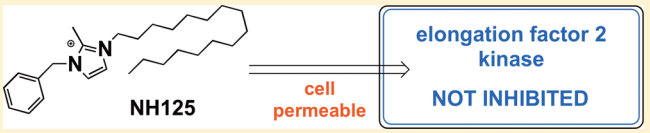

eEF-2K (eukaryotic elongation factor 2 kinase, also known as calcium/calmodulin-dependent protein kinase III) is an atypical serine/threonine specific protein kinase whose catalytic domain has no sequence similarity to conventional protein kinases.[1,2] To date, its only known substrate of physiological relevance is eEF2 (eukaryotic elongation factor 2), a ribosome binding protein that facilitates the translocation of the ribosome along mRNA during translation.[3,4] Although its structure is not yet available, mutational studies have confirmed that the eEF-2K polypeptide consists of an N-terminal catalytic domain connected via a linker to a C-terminal domain that is important for eEF2 binding.[2] eEF-2K phosphorylates eEF2 mainly at Thr-56 and Thr-58 within the sequence ^{50}RAGETRFT*DT*RKD^{62}.[5] Phosphorylation of eEF2 decreases the affinity of eEF2 for the ribosome, leading to inhibition of protein synthesis.[6−8]

In recent years, eEF-2K has been associated with autophagy, a process favoring cancer cell survival. For example, in glioblastoma cell lines, the overexpression of eEF-2K is reported to enhance autophagy, while siRNA-mediated depletion of eEF-2K is reported to decrease autophagy, as measured by the formation of LC3-II, formation of acidic vesicular organelles (AVOs), and electron microscopy.[9,10] A mechanistic understanding of how eEF-2K may regulate autophagy remains to be determined. In normal cells, autophagy is considered a survival mechanism under conditions of nutrient deprivation.[11,12] Many cancer cells also induce autophagy in response to anticancer therapies such as radiation therapy, hormonal therapy, and chemotherapy.[13−28] Therefore,

Received: December 5, 2011
Revised: February 12, 2012
Published: February 21, 2012

dx.doi.org/10.1021/bi201787p | Biochemistry 2012, 51, 2100−2112

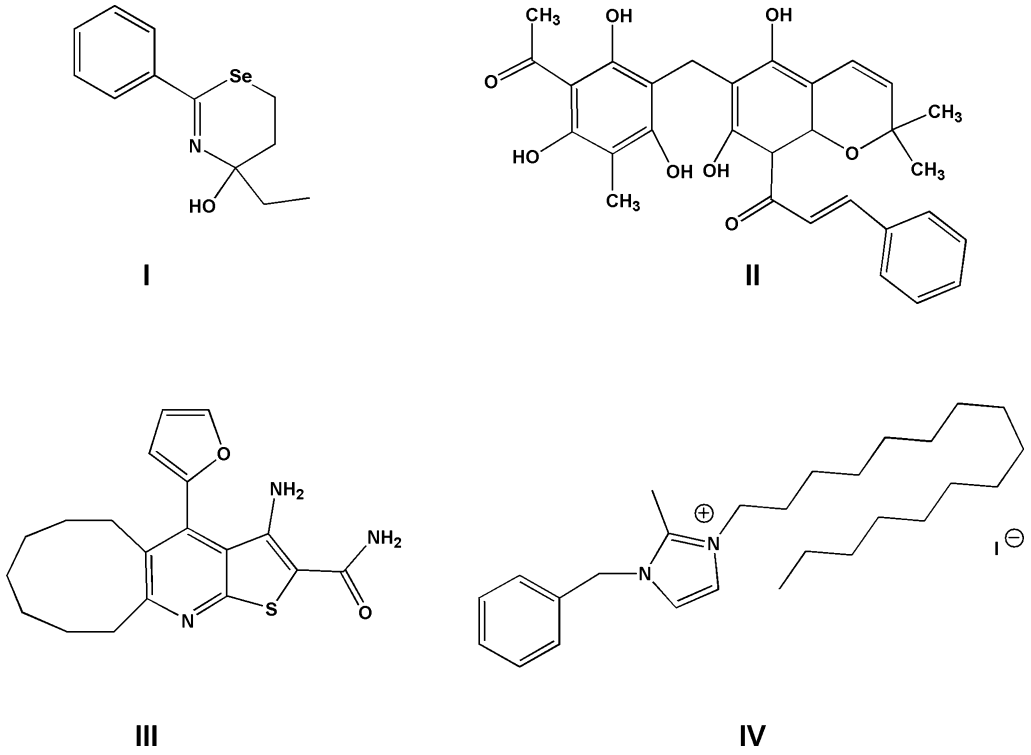

Figure 1. Known eEF-2K inhibitors. 1,3-Selenazine (**1**) is a potent ATP-competitive inhibitor of eEF-2K and is reported to block the phosphorylation of eEF2 in cells at a concentration of 20 μM but is unstable to thiols.[37] Rottlerin (**2**) is a nonspecific inhibitor of multiple protein kinases.[63,64] Thieno[2,3-*b*]pyridine (**3**) is an ATP-competitive inhibitor of eEF-2K that lacks potency in cells.[39] The mechanism of inhibition of NH125 (**4**), which was first identified as a histidine kinase inhibitor[50,65] and later as an inhibitor of eEF-2K,[40] has not been determined.

it has been postulated that eEF-2K may promote cancer cell survival by regulating autophagy, suggesting that eEF-2K may be a candidate for targeted cancer therapy.[9,10,29]

The activity of eEF-2K is increased in fresh human tumor samples and several cancer cell lines.[9,10,30−34] Its activity is also greater in proliferating cells,[32,34,35] especially during the S phase of the cell cycle.[30,36] Recently, we discovered that eEF-2K enhances a number of processes associated with tumorigenesis through its effects on multiple signaling pathways and provided the first evidence that in vivo therapeutic targeting of eEF-2K expression inhibits growth of established tumors in an orthotopic xenograft model of a highly aggressive and metastatic breast cancer.

Several pharmacological inhibitors of eEF-2K have been described in the literature (Figure 1). These include the 1,3-selenazine derivative (**1**),[37] rottlerin (**2**),[34,38] the thieno[2,3-*b*]pyridine derivative (**3**),[39] and histidine kinase inhibitor NH125 (**4**).[40] NH125 has been used by a number of investigators to investigate eEF-2K activity in cell cultures.[40−44] However, while NH125 is reported to inhibit GST-eEF-2K with an IC_{50} of 60 nM,[40] its mechanism of inhibition has not been reported.

An understanding of the mechanism and regulation of eEF-2K has been hampered by the lack of a reliable source of the kinase. However, we recently reported the expression and purification of human eEF-2K using a bacterial expression system.[45] The resulting preparation is highly active, monomeric, and suitable for detailed mechanistic studies. The goal of this work was to first delineate the kinetic mechanism of peptide phosphorylation by eEF-2K and then to assess the mechanism by which NH125 inhibits the kinase. The kinetic analysis revealed an ordered mechanism in which ATP must bind before the peptide substrate to form a productive ternary complex. Upon investigating the mechanism with NH125, we found that its ability to inhibit eEF-2K was prevented by the addition of a small amount of detergent, a hallmark of a nonspecific aggregator.[46−48] In a subsequent in vitro assay, 0−5 μM NH125 failed to inhibit the phosphorylation of wheat germ EF2 by eEF-2K. Similar effects were observed in cellular studies using MDA-MB-231 breast cancer, A549 lung cancer, and HEK-293T cell lines, where treatment with 4 μM NH125 for 12 h did not inhibit eEF-2 phosphorylation. Instead, NH125 treatment led to an increase in the levels of phospho-eEF2 in all of the tested cell lines. The ability of NH125 to induce phosphorylation of eEF-2 was also recently reported by Chen et al.[49] using H1299 (non-small cell lung carcinoma), PC3 (prostate cancer), HeLa (cervical cancer), H460 (non-small cell lung carcinoma), and C6 (rat glioma) cell lines. Together, these data support the notion that NH125 is not a cellular inhibitor of eEF-2K.

MATERIALS AND METHODS

Buffers and Reagents. Competent cells used for amplification and expression were provided by Novagen (Gibbstown, NJ). Yeast extract and tryptone were purchased from US biological (Swampscott, MA). IPTG and DTT were obtained from USB (Cleveland, OH). All buffer components used in the protein expression, purification, and enzyme assays, including HEPES, Trizma base (Tris), sodium chloride, potassium chloride, EDTA, EGTA, calcium chloride, magnesium chloride, Brij-35, Triton X-100, β-mercaptoethanol, DTT, benzamidine hydrochloride, TPCK, and PMSF, were ultrapure grade and were purchased from Sigma (St. Louis, MO). Ni-NTA agarose was supplied by Qiagen (Santa Clara, CA).

dx.doi.org/10.1021/bi201787p | *Biochemistry* 2012, 51, 2100−2112

Amersham Biosciences (Pittsburgh, PA) provided the FPLC system and the columns for purification. P81 cellulose papers were obtained from Whatman (Piscataway, NJ). ATP was purchased from Roche (Indianapolis, IN). Radiolabeled [γ-^{32}P]ATP was obtained from Perkin-Elmer (Waltham, MA). ADP was from MP Biomedicals (Solon, OH).

Enzyme Expression and Purification. Methods for eEF-2K and calmodulin purification have been described previously.[45]

Peptide Synthesis. Peptide substrate (Pep-S, acetyl-RKKYKFNEDTERRRFL-amide) and peptide inhibitor (Pep-I, acetyl-RKKYKFNEDAERRRFL-amide) were synthesized and purified by HPLC at the Institute for Cell and Molecular Biology at The University of Texas. The peptides were raised in 25 mM HEPES (pH 7.5) and were verified by MALDI. The concentration was determined on the basis of the absorbance at 280 nm (OD_{280}) using an extinction coefficient of 1280 cm^{-1} M^{-1} and a path length of 1 cm.

Two-Substrate Kinetic Assay. Assays were performed in a 100 μL volume at 30 °C in assay buffer [25 mM HEPES (pH 7.5), 50 mM KCl, 0.1 mM EDTA, 0.1 mM EGTA, 2 mM DTT, 1.5 mM $CaCl_2$, 10 mM $MgCl_2$, 1 μM CaM, and 40 μg/mL BSA] containing 10 nM eEF-2K, 0−1000 μM [γ-^{32}P]ATP (specific activity of 1000 cpm/pmol), and 0−720 μM Pep-S (acetyl-RKKYKFNEDTERRRFL-amide). Reaction mixtures were prepared and kept on ice until the time of the assay. Reaction mixtures were incubated for 10 min at 30 °C, and the reactions were started with the addition of [γ-^{32}P]ATP. Aliquots (10 μL) were taken and spotted onto P81 cellulose papers at fixed time point intervals. The papers were washed with 50 mM phosphoric acid (five times for 10 min each) and then dried following an acetone wash. The amounts of radiolabeled phosphopeptides were determined by counting the associated counts per minute on a scintillation counter (Packard 1500) at a σ value of 2. eFF-2K requires the binding of calmodulin and the autophosphorylation of Thr-348 to achieve full activity.[66] Under the conditions of the kinetic experiments, all plots of product versus time are linear. Observed rates were independent of the order of addition of substrates.

Product and Dead-End Inhibition Assay. Inhibition assays with product ADP or the dead-end peptide inhibitor (Pep-I, acetyl-RKKYKFNEDAERRRFL-amide) were conducted as described above. First, the ATP concentration was varied (12.5−125 μM) with the Pep-S concentration fixed at 50 μM. Then, the Pep-S concentration was varied (15−90 μM) with the ATP concentration fixed at 50 μM. The concentrations used in the inhibition assays for ADP were 0−4 mM and for Pep-I were 0−500 μM.

Synthesis of 1-Benzyl-3-cetyl-2-methylimidazolium Iodide (NH125). NH125 was synthesized according to the reported procedure[50] with some modifications.

Synthesis of Cetyl-2-methylimidazole. 2-Methylimidazole (10 g, 122 mmol, 10 equiv) in chloroform (150 mL) was stirred for 10 min at 70 °C. Bromohexadecane (7.46 mL, 12.2 mmol, 1 equiv) in chloroform (15 mL) was added dropwise to the solution described above and refluxed overnight while being stirred. A large excess of 2-methylimidazole was used to prevent the unfavorable doubly alkylated side product formation. The reaction mixture was dissolved with water (1 L, to remove excess 2-methylimidazole), and the organic layer was extracted with EtOAc (3 × 50 mL). The combined organic layer was washed with water (3 × 50 mL) and dried with $MgSO_4$, and the solvent was evaporated under vacuum to obtain the crude product. After purification by flash chromatography (10:1 chloroform/methanol), the product was obtained as an off-white powder (2.7 g, 72%).

Synthesis of 1-Benzyl-3-cetyl-2-methylimidazolium Iodide (NH125). Potassium iodide (14.18 g, 10 equiv) and benzyl bromide (2.92 g, 17.08 mmol, 2 equiv) in chloroform (100 mL) were refluxed for 15 min. Cetyl-2-methylimidazole (2.62 g, 8.54 mmol, 1 equiv) in chloroform (40 mL) was added dropwise to the solution described above and refluxed overnight. Solvent was evaporated under vacuum to obtain the crude product. After purification by flash chromatography (7:1 chloroform/methanol) and recrystallization using ethyl acetate, the product was obtained as a white solid (1.74 g, 52.4%): ^{1}H NMR (400 MHz, DMSO-d_6) δ 7.72 (s, 2H), 7.43−7.33 (m, 3H), 7.3 (d, 2H, J = 6.4 Hz), 5.39 (s, 2H), 4.1 (t, 2H, J = 7.2 Hz), 2.60 (s, 3H), 1.71 (br, 2H), 1.21 (br, 26H), 0.83 (t, 3H, J = 6.8 Hz); ^{13}C NMR (100.6 MHz, DMSO-d_6) δ 144.76, 135.0, 129.44, 128.92, 128.13, 122.13, 122.03, 51.03, 48.11, 31.73, 29.49, 29.45, 29.39, 29.36, 29.31, 29.15, 26.06, 22.54, 14.41, 9.94 (some C's are overlapping); ESI-MS [M + H]$^+$ calcd 397.357, observed 397.5.

In Vitro Assays with NH125. NH125 was synthesized, and its identity and purity were verified by ESI-MS and NMR (Figures S1 and S2 of the Supporting Information). Dose−response inhibition assays against eEF-2K were performed using 2 nM eEF-2K, 50 μM [γ-^{32}P]ATP, 30 μM Pep-S, and various concentrations of NH125 (0−100 μM). To test the sensitivity against detergent, the same assays described above were also performed in the presence of 0.1% Triton X-100. Similarly, competition assays were conducted using 2 nM eEF-2K, 30 μM Pep-S, and varying concentrations of NH125 (0−100 μM) at different fixed concentrations of [γ-^{32}P]ATP (50 μM or 2 mM). In all cases, the enzyme was preincubated with [γ-^{32}P]ATP for 15 min before the reaction was initiated with NH125 and Pep-S. Assay buffer for eEF-2K contained 25 mM HEPES (pH 7.5), 50 mM KCl, 0.1 mM EDTA, 0.1 mM EGTA, 150 μM $CaCl_2$, 1 μM CaM, 40 μg/mL BSA, 2 mM DTT, 10 mM $MgCl_2$, and 5% DMSO. The $CaCl_2$ concentration used in these assays is 10-fold lower than in the two-substrate kinetic assays described above. Under these conditions, the activity of eEF-2K is slightly higher; however, this has no effect on the IC_{50} for NH125. To test the specificity of NH125, dose−response inhibition assays were also performed against TRPM7 and ERK2. Dose−response assays against ERK2 were performed using 2 nM ERK2, 500 μM [γ-^{32}P]ATP, 20 μM Ets1, and various concentrations of NH125 (0−500 μM). Dose−response assays against TRPM7 were performed using 25 nM TRPM7, 500 μM [γ-^{32}P]ATP, 20 μM TRPM7 peptide (Ac-RKKYRIVWKSIFRRFL-NH_2), and various concentrations of NH125 (0−500 μM). Assay buffer for TRPM7 and ERK2 contained the same components as that of eEF-2K without calcium or calmodulin.

Effect of NH125 on eEF2 Phosphorylation. Purification of wheat germ EF2 has been described previously.[51] Assays were performed at 30 °C in assay buffer [25 mM HEPES (pH 7.5), 50 mM KCl, 0.1 mM EDTA, 0.1 mM EGTA, 150 μM $CaCl_2$, 1 μM CaM, 40 μg/mL BSA, 2 mM DTT, 10 mM $MgCl_2$, and 5% DMSO] containing 10 nM eEF-2K, 1 μM eEF2, 7.5 μM ATP, and different concentrations of NH125 (0, 50, 500, and 5000 nM). Assay buffer containing eEF-2K (10 nM) and wheat germ EF2 (1 μM) were preincubated for 30 min in the presence of the concentrations of NH125 listed

above. Then the assays were started with the addition of [γ-^{32}P]ATP. Reactions were allowed to proceed for 10 min and quenched by addition of sodium dodecyl sulfate−polyacrylamide gel electrophoresis (SDS−PAGE) sample loading buffer, and then the mixtures were heated for 10 min at 95 °C. We made sure that the assay rate after 10 min corresponded to the initial rate of the reaction. The quenched samples were resolved by running in 10% SDS−PAGE and staining with Coomassie Brilliant Blue dye. Once the gel had been dried, the bands corresponding to phospho-EF2 were excised and the associated counts were quantified on a scintillation counter (Packard 1500) at a σ value of 2.

Cell Lines and Culture Conditions. HEK 293T, MDA-MB-231 (breast adenocarcinoma), and A549 (lung carcinoma) cell lines were all obtained from American Type Culture Collection (Manassas, VA). The HEK 293T cell line was cultured in DMEM, while MDA-MB-231 and A549 cells were cultured in DMEM/F12. Both media were supplemented with 10% FBS, 50 units/mL penicillin, and 50 μg/mL streptomycin. Cell cultures were maintained at 37 °C in a humidified incubator containing 5% CO_2. All cell culture reagents were from Invitrogen.

Commercial Antibodies. The following antibodies were purchased from Cell Signaling Technology (Danvers, MA): anti-phospho-eEF2 (Thr56) antibody (catalog no. 2331, 1:2000), anti-eEF2 antibody (catalog no. 2332, 1:2000), anti-eEF-2K antibody (catalog no. 3692, 1:2000), and anti-mouse IgG, HRP-linked antibody (catalog no. 7076, 1:2000). Anti-Actin, clone C4 antibody (MAB1501, 1:10000) was obtained from Millipore (Billerica, MA), and goat anti-rabbit IgG (H+L)−HRP conjugate (catalog no. 172-1019, 1:2000) was from Bio-Rad (Hercules, CA).

Treatment of Cells with NH125. For analysis of the effects of NH125 on phosphorylated eEF2 levels in cells, cells were seeded in six-well plates at a density of 0.8×10^6 cells per well in 2 mL of medium. After 36 h, cells were treated with 4 μM NH125 (with a final DMSO concentration of 0.1%) for 0, 3, 6, and 12 h. Cells in the control wells were treated with DMSO (final concentration of 0.1%) for the same lengths of time.

Western Blot Analysis. Following treatments, cells were washed twice in PBS (pH 7.4) (Invitrogen) and lysed in ice-cold M-PER Mammalian Protein Extraction Reagent (Thermo Fisher Scientific, Rockford, IL) containing Halt Protease and Phosphatase Inhibitor (Thermo Fisher Scientific). Lysates were clarified by centrifugation at 15000g for 15 min. Total protein concentrations for each sample were determined by the Bradford assay (Bio-Rad). Equal amounts of protein (7.5 μg) from cell lysates were resolved by 10% SDS−PAGE and were transferred to Amersham Hybond-P PVDF membranes (GE Healthcare, Piscataway, NJ). Membranes were blocked with 5% nonfat dry milk in a Tris-buffered saline/Tween 20 mixture (TBST) and incubated with primary antibody anti-phospho-eEF2 (Thr56), anti-eEF2, or anti-eEF-2K at 4 °C overnight. The membranes were washed with TBST and incubated with the secondary antibody goat anti-rabbit IgG (H+L)−HRP conjugate at room temperature for 2 h. To determine the total levels and phosphorylation status of specific proteins, we performed chemiluminescent detection with Amersham ECL Plus Western Blotting Detection Reagents (GE Healthcare). Anti-actin, clone C4 and anti-mouse IgG, HRP-linked antibodies were used to monitor total actin levels as a loading control.

Data Analysis. Initial velocity data for substrate and inhibition kinetics were fitted globally using a nonlinear least-squares approach using Scientist (Micromath). For some fitting, Kaliedagraph 3.5 (Synergy Software) was used. Initial rate data were fit globally to eq 1, which describes a mechanism of competitive substrate inhibition through a dead-end EB complex (see eq IX-384 on page 819 of ref 52). The initial rate data displaying competitive, uncompetitive, and mixed-type inhibition patterns at subsaturating concentrations of cosubstrates were fit globally to eqs 2−4 respectively.[52] A slope replot describing a mechanism of competitive substrate inhibition through a dead-end EB complex was fit to eq 5 (see eq IX-386 on page 821 of ref 52). An intercept replot describing a mechanism of competitive substrate inhibition through a dead-end EB complex was fit to eq 6 (see Figure IX-61 on page 821 of ref 52). A slope replot at different fixed concentrations of Pep-I was fit to eq 7 (see eq IV-16 on page 173 of ref 52). Dose−response IC_{50} curves were fit using eq 8.[53]

$$v = (V_{max}[A][B])/[K_{ia}K_{mB}(1 + [B]/K_{iB}) + K_{mA}[B](1 + [B]/K_{iB}) + K_{mB}[A] + [A][B]] \quad (1)$$

$$v = \frac{V_{max}^{app}[S]}{K_{mS}^{app}(1 + [I]/K_{iC}^{app}) + [S]} \quad (2)$$

$$v = \frac{V_{max}^{app}[S]}{K_{mS}^{app} + [S](1 + [I]/K_{iU}^{app})} \quad (3)$$

$$v = \frac{V_{max}^{app}[S]}{K_{mS}^{app}(1 + [I]/K_{iC}^{app}) + [S](1 + [I]/K_{iU}^{app})} \quad (4)$$

$$\text{slope}_{1/A} = \frac{K_{mA}}{V_{max}K_{iB}}[B] + \frac{K_{iA}K_{mB}}{V_{max}}[B]^{-1} + \frac{K_{mA}}{V_{max}}\left(1 + \frac{K_{iA}K_{mB}}{K_{mA}K_{iB}}\right) \quad (5)$$

$$\frac{1}{V_{max}^{app}} = \frac{K_{mB}}{V_{max}}\frac{1}{[B]} + \frac{1}{V_{max}} \quad (6)$$

$$\text{slope}_{1/A} = \frac{K_{mA}^{app}}{V_{max}^{app}K_{iC}^{app}}[I] + \frac{K_{mA}^{app}}{V_{max}^{app}} \quad (7)$$

$$v_i = \frac{v_0}{(1 + [I]/IC_{50})^h} \quad (8)$$

where v is the observed velocity, V_{max} the maximal initial velocity, [A] the concentration of substrate A, [B] the concentration of substrate B, K_{iA} the dissociation constant for substrate A, K_{mA} the Michaelis−Menten constant for substrate A, K_{mB} the Michaelis−Menten constant for substrate B, K_{iB} the inhibition constant for the EB complex, [S] the concentration of varied substrate S, K_{mS} the apparent Michaelis−Menten constant for substrate S, [I] the concentration of inhibitor I, K_{iC} the inhibition constant for the EI (enzyme−inhibitor) complex, K_{iU} the inhibition constant for the ESI complex, v_i the observed velocity in the presence of inhibitor, v_0 the observed velocity in the absence of inhibitor, IC_{50} the inhibitor concentration required to achieve 50% inhibition, and h the Hill coefficient. Apparent kinetic constants obtained at subsaturating substrate

dx.doi.org/10.1021/bi201787p | Biochemistry 2012, 51, 2100−2112

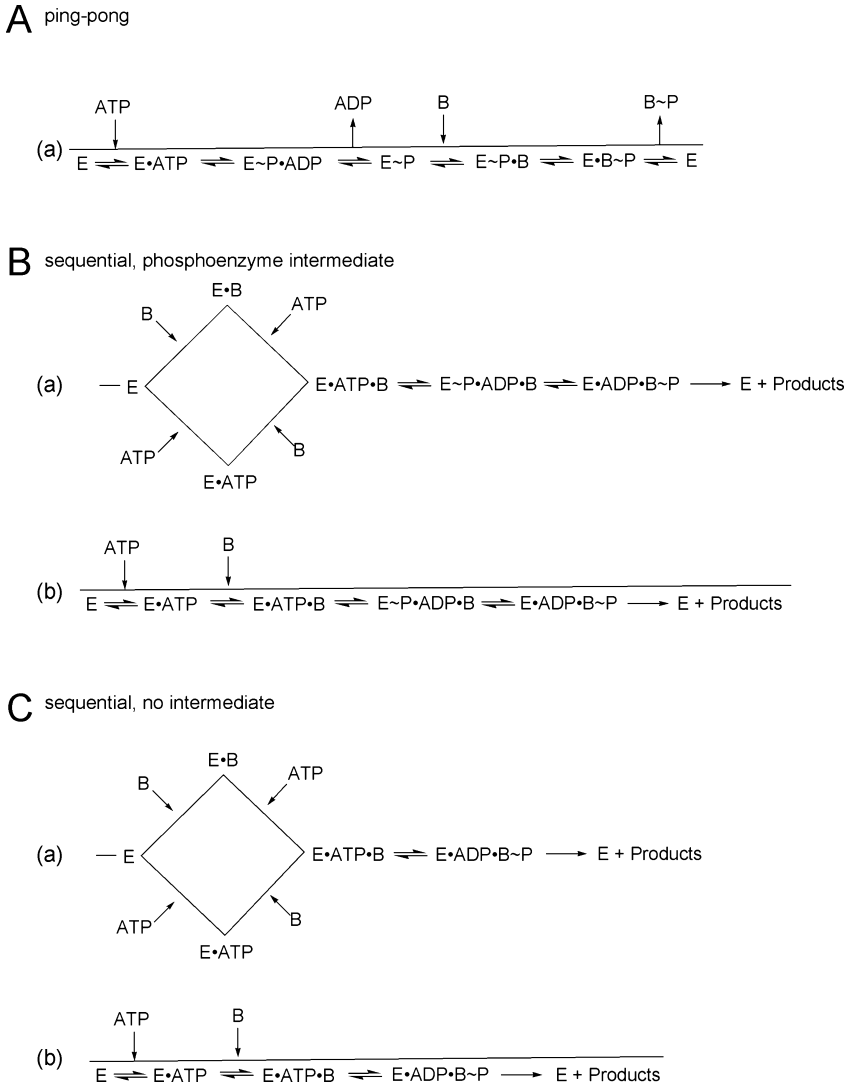

Figure 2. Bisubstrate kinetic mechanisms. (A) Ping-pong mechanism with a phospho-enzyme intermediate. (B) Sequential mechanisms with a phospho-enzyme intermediate: (a) random-order sequential mechanism and (b) ordered sequential mechanism with ATP binding first. (C) Sequential mechanisms with no phospho-enzyme intermediate: (a) random-order sequential mechanism and (b) ordered sequential mechanism with ATP binding first.

concentrations are designated by app, for example, V_{max}^{app}, K_m^{app}, K_{iC}^{app}, and K_{iU}^{app}.

RESULTS

A recent structural study of the *Dictyostelium* protein kinase myosin heavy chain kinase suggested a possibly catalytic mechanism through a phosphoprotein intermediate.[54] As MHCK is an atypical protein kinase that is predicted to be structurally similar to eEF-2K (33% identical sequence in the catalytic domain), we were interested in the possibility that eEF-2K catalyzes the transfer of a phosphoryl group to the peptide through a phosphoenzyme intermediate. eEF-2K is reported to phosphorylate the peptide RKKFGEAEKT*KAKEFL, with a K_m^{app} of 580 μM.[55] Here we have utilized a similar peptide, Ac-RKKYKFNEDT*ERRRFL-NH_2 (Pep-S), to assay the activity of eEF-2K.[45] Both peptides contain a basic residue at the position 3, which is reported to be important for efficient peptide phosphorylation by eEF-2K[55] and corresponds to the Arg residue in position 3 relative to Thr-56, the major phosphorylation site in eEF2.[5] To define the basic kinetic mechanism, we examined the dependence of product formation on the concentrations of substrates by the method of initial rates.[52] The appearance of product with time was linear under all experimental conditions and was highly reproducible, to within 10%.

Sequential or Ping-Pong Kinetics. To explore the possibility of a phospho-enzyme intermediate we examined whether eEF-2K phosphorylates Pep-S through a ping-pong mechanism whose reciprocal plot exhibits a characteristic family of parallel lines (mechanism A in Figure 2). According to this mechanism, MgATP binds the enzyme, E, and reacts to form the phospho-intermediate, E~P, and MgADP. MgADP dissociates before B binds E~P. Subsequent phospho transfer gives B~P, which then dissociates from E. Initial rate studies were performed using ATP (0−1000 μM) and the peptide Ac-RKKYKFNEDTERRRFL-NH_2 (Pep-S) (0−720 μM). Because of substrate inhibition at high peptide concentrations (described below), analysis of double-reciprocal plots was performed at low peptide concentrations (0−90 μM). The double-reciprocal plots of $1/v$ versus $1/[ATP]$ (Figure 3A) and $1/v$ versus $1/[Pep-S]$ (Figure 3B) converge to the left of the $1/$

dx.doi.org/10.1021/bi201787p | *Biochemistry* 2012, 51, 2100−2112

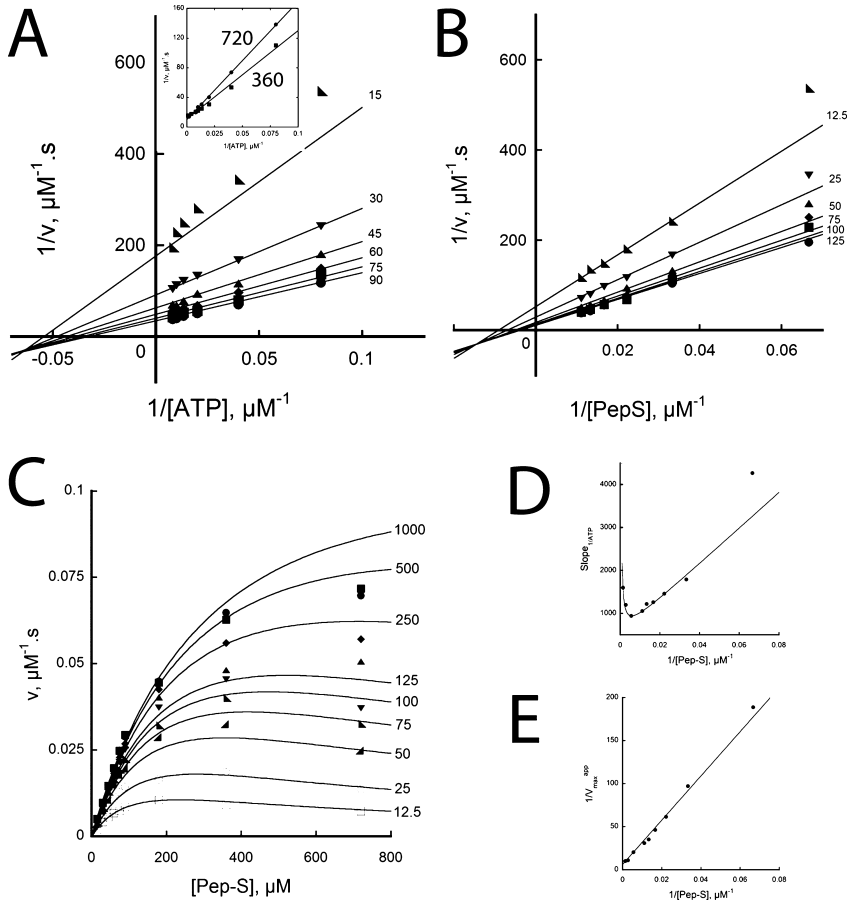

Figure 3. Dependence of reaction velocities on substrate concentration. Initial velocities were measured using 10 nM eEF-2K. (A) $1/v$ vs $1/[ATP]$. Initial velocities were measured using several fixed concentrations of Pep-S (as indicated in micromolar) and varied concentrations of ATP (12.5−125 μM). The inset shows $1/v$ vs $1/[ATP]$ for 360 and 720 μM Pep-S showing intersection at $1/V_{max}^{app}$. (B) $1/v$ vs $1/[Pep-S]$. Initial velocities were measured using several fixed concentrations of ATP (as indicated in micromolar) and varied concentrations of Pep-S (15−90 μM). The lines correspond to the best fit to eq 1 according to the parameters in Table 1. (C) Velocity, v, vs [Pep-S]. Initial velocities were measured using several fixed concentrations of ATP (as indicated in micromolar) and varied concentrations of Pep-S (15−720 μM). The lines correspond to the best fit to eq 1 according to the parameters in Table 1. (D) Slope replot of panel A. The line corresponds to the best fit to eq 5 according to the parameters in Table 1. (E) Intercept replot of panel A. The line corresponds to the best fit to eq 6 according to the parameters in Table 1.

v axis. Such patterns of convergent lines are not consistent with a ping-pong mechanism (Figure 2A); rather, they are consistent with sequential mechanisms in which both substrates must bind before any product dissociates (e.g., mechanisms B and C in Figure 2). While a sequential mechanism does not rule out a kinetically significant phospho-enzyme intermediate, it requires that ADP cannot dissociate from the enzyme until after Pep-S is bound. Mechanism B in Figure 2 shows two possible sequential mechanisms that conform to such a restriction.

Substrate Inhibition. When analyzing the velocity dependence of eEF-2K on substrates, we noted that at higher concentrations of Pep-S its velocity decreases with an increasing Pep-S concentration (Figure 3C). In contrast, MgATP exhibits a normal saturation dependence with an increasing concentration and does not inhibit the enzyme. In general, substrate inhibition occurs when substrates add to the wrong enzyme form and usually becomes evident at high substrate concentrations. As it can often provide additional mechanistic insight, we decided to determine its mechanism. To evaluate substrate inhibition of eEF-2K by Pep-S, the dependencies of the slope ($slope_{1/ATP}$) and $1/V_{max}^{app}$ of the lines in Figure 3A were first assessed as a function of $1/[Pep-S]$. Figure 3D shows that the slope ($slope_{1/ATP}$) decreases, passes through a minimum, and then increases as $1/[Pep-S]$ decreases. In contrast, $1/V_{max}^{app}$ decreases linearly and intercepts the ordinate at $1/V_{max}$ (Figure 3E). These data are consistent with a mechanism in which Pep-S competitively inhibits MgATP.[52] Two possible mechanisms that can account for such competitive substrate inhibition are shown in Figure 4. According to the mechanism shown in Figure 4A, the binding of Pep-S (B) prevents the binding of ATP within the active site; therefore, MgATP must bind the enzyme before Pep-S.[52] In the mechanism shown in Figure 4B, ATP is prevented from binding the active site when Pep-S (B) binds the enzyme, E, at a second site. In both cases, Pep-S is competitive with ATP binding, and inhibition can be overcome by high concentrations of MgATP. The most significant difference between the two mechanisms is that in mechanism 4B the peptide binds two sites on the enzyme, whereas in mechanism 4A there is only one. It should be noted that the data in Figure 3C are fit globally to eq 1, which describes the mechanism in Figure 4A. The parameters for the best fit are given in Table 1. Further support for this mechanism is presented below.

To further assess the mechanism, we performed kinetic experiments at different fixed concentrations of Pep-I and ADP. Pep-I has the same sequence, Ac-RKKYKFNEDA*ERRRFL-

dx.doi.org/10.1021/bi201787p | Biochemistry 2012, 51, 2100−2112

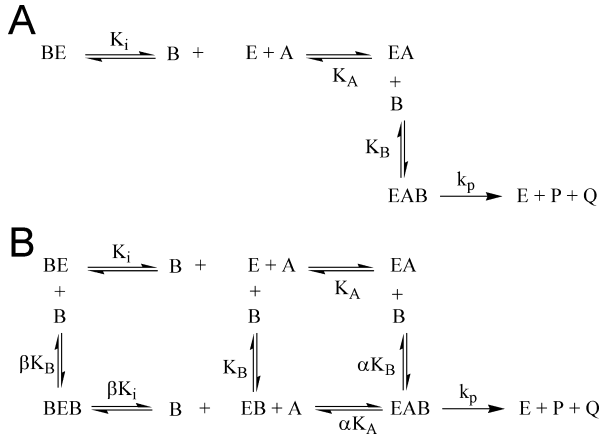

Figure 4. Possible mechanisms of competitive substrate inhibition by Pep-S. (A) Pep-S (B) binds E to form an abortive complex incapable of binding ATP. (B) The binding of Pep-S (B) to a second binding site on E inhibits the binding of ATP.

Table 1. Kinetic Parameters for the Phosphorylation of Pep-S by eEF-2K[a]

V_{max}	0.15 ± 0.01 μM/s
K_{ia}	16.2 ± 6.9 μM
K_{mA}	36.5 ± 3.5 μM
K_{mB}	393 ± 40 μM
K_{iB}	178 ± 16 μM

[a]The parameters were obtained from global fitting of the kinetic data in Figure 3C for substrate phosphorylation to eq 1.

NH_2, which is identical to that of Pep-S, except for a threonine to alanine substitution; thus, it may be considered a dead-end inhibitor that binds eEF-2K in a manner similar to that of Pep-S. ADP is a product of the kinase reaction and is expected to bind eEF-2K in a manner similar to that of ATP. ADP exhibits competitive inhibition with respect to ATP (Figure 5A) and exhibits mixed-type inhibition with respect to Pep-S (Figure 5B). Pep-I exhibits competitive inhibition toward Pep-S (Figure 5C) and mixed-type inhibition toward ATP (Figure 5D). This pattern of inhibition (Figure 5; summarized in Table 2) is consistent with either mechanism shown in Figure 4. However, if it is assumed that Pep-S (B) and Pep-I (I) bind eEF-2K in a similar manner, and that Pep-I can be substituted for Pep-S in Figure 4, the two mechanisms may be differentiated on the basis that mechanism A involves the binding of one molecule of Pep-I to eEF-2K while mechanism B involves the binding of two molecules of Pep-I. The linear plot of $slope_{1/ATP}$ versus [Pep-I] over the range of 0−500 μM Pep-I (Figure 5E) supports the notion that eEF-2K phosphorylates Pep-S through mechanism A,[52] because such a plot is expected to be nonlinear for mechanism B. The lines through the data correspond to the best fit to the appropriate equations as described in the legend of Figure 5.

Inhibition of eEF-2K. 1-Benzyl-3-hexadecyl-2-methyl-1*H*-imidazol-3-ium iodide (NH125) (**4** in Figure 1) is reported to specifically inhibit eEF-2K with an IC_{50} of 60 nM in an in vitro kinase assay.[40] It is also reported to decrease the level of eEF2 phosphorylation in cells[40−44] and to decrease the viability of a number of cancer cell lines with EC_{50} values of ∼1−5 μM.[40] However, its mechanism of inhibition has not been demonstrated. Therefore, we decided to evaluate the mechanism of inhibition of eEF-2K by NH125. We synthesized an authentic sample of NH125 (see Materials and Methods) and confirmed its structure by mass spectrometry, ^1H NMR, and ^{13}C NMR (see Figures S1 and S2 of the Supporting Information). The ability of NH125 to inhibit eEF-2K was assessed using the same in vitro kinase assay as described above. Dose−response curves for NH125 were obtained at several concentrations of ATP to evaluate whether NH125 competes with the ATP binding site on the enzyme. If NH125 competed with ATP, a right shift in the dose−response curve would be expected as the concentration of ATP is increased. Figure 6A shows a dose−response curve exhibiting a steep dependence on the concentration of NH125 (Hill coefficient of 3.7). Dose−response curves obtained at 50 and 2000 μM are essentially superimposable (Figure 6B), suggesting that NH125 does not compete with ATP. Similar results were observed when two concentrations of the peptide substrate (10 and 100 μM) were used (Figure 6C), and a 20-fold increase in the concentration of calmodulin from 0.1 to 2 μM resulted in a slight (<2-fold) increase in the observed IC_{50} (data not shown). Notably, the IC_{50} of ∼18 μM obtained in these experiments is 300-fold higher than the previously reported value of 60 nM. As the presence of small amounts of nonionic detergents can often attenuate the effects of compounds acting as nonspecific aggregators,[46−48] assays were performed in the presence (0.1%) or absence of Triton X-100 to test the possibility that NH125 is an aggregator. Increasing the concentration of Triton X-100 from 0 to 0.1% clearly resulted in an increase in the magnitude of the observed IC_{50} from 18 to 452 μM (Figure 6A). When NH125 was assessed against TRPM7 (a related protein kinase) and ERK2 (an unrelated protein kinase), it was also found to inhibit both kinases with IC_{50} values of 55 and 70 μM and Hill coefficients of 1.6 and 3.6, respectively (data not shown). Taken together, these data suggest that NH125 is a nonspecific colloidal aggregator.[46−48] Because NH125 is reported to potently inhibit the phosphorylation of eEF2, we tested the effect of NH125 (0−5 μM) on the phosphorylation of wheat germ eEF2 by eEF-2K in vitro. As seen in Figure 6D, NH125 (0−5 μM) has no detectable effect on the rate of phosphorylation of eEF2 (1 μM) in the presence of ATP (7.5 μM) (see Materials and Methods), consistent with the kinetic analysis with the peptide. As predicted, inhibition is observed at higher concentrations of NH125 (12.5−50 μM) (Figure S3 of the Supporting Information). In summary, a steep Hill coefficient, an absence of competition against ATP or peptide, and a lack of specificity are consistent with NH125 being a promiscuous aggregator.[46−48] The observed rate of decay of the autocorrelation function of a solution of 50 μM NH125 measured by dynamic light scattering provides further support for the presence of aggregate material. Comparison with a solution of tetraiodophenolphthalein, which forms aggregates approximately 150 nm in diameter,[46] suggests that NH125 forms relatively smaller particles (data not shown). Further characterization of the particulate properties of NH125, which is not the focus of this work, is underway.

To examine whether the activity of NH125 was associated with the downregulation of eEF2 phosphorylation, we examined the ability of 4 μM NH125 to affect the phosphorylation of eEF2 on Thr-56 in MDA-MB-231 breast cancer, A549 lung cancer, and HEK-293T cell lines over a period of 0−12 h (Figure 7). The levels of expression of eEF2, eEF-2K, and actin were also assessed. Contrary to previous reports,[40−44] we observed no signs of decrease in the phospho-eEF2 levels in the presence of NH125 in any of the tested cell

dx.doi.org/10.1021/bi201787p | *Biochemistry* 2012, 51, 2100−2112

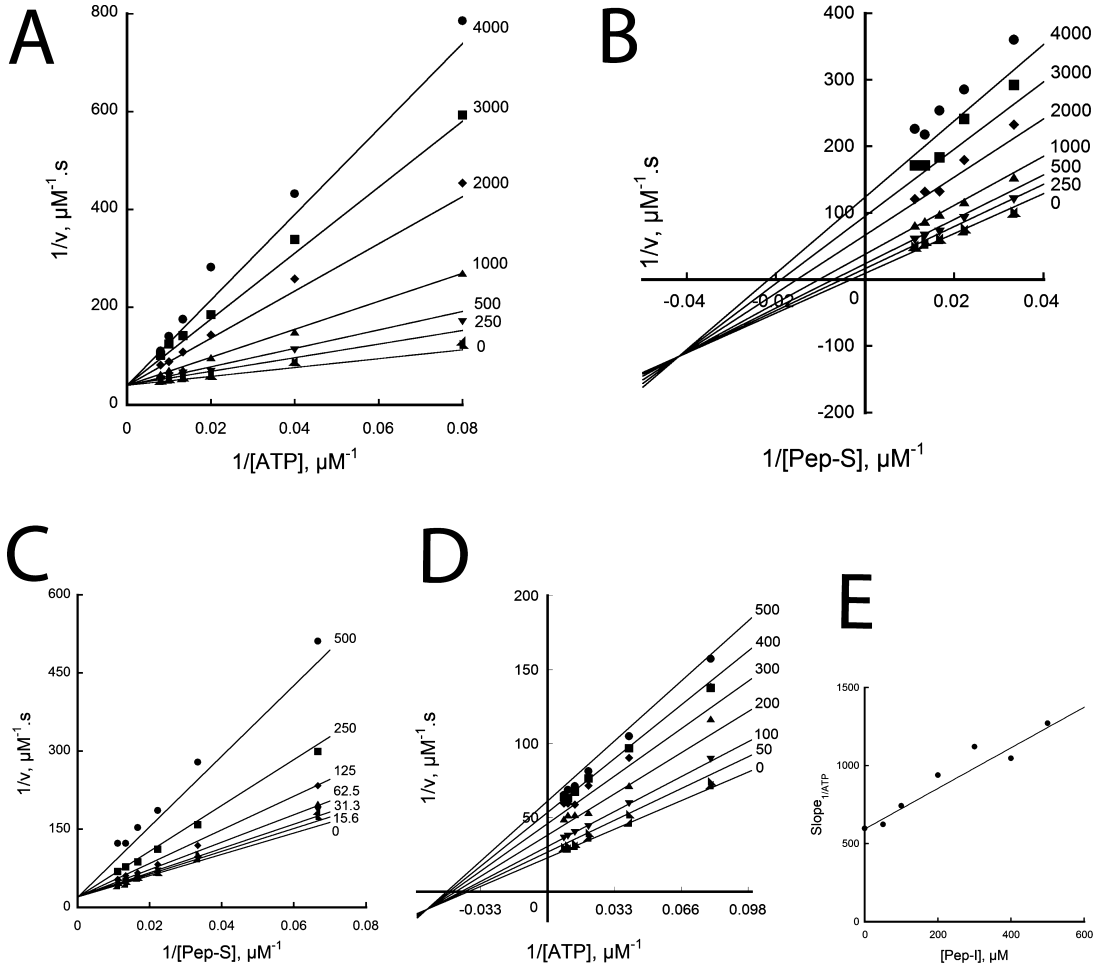

Figure 5. Dependence of reaction velocities on ADP and Pep-I. (A) Competitive inhibition of ADP toward ATP. Initial velocity studies at 50 μM Pep-S in the presence of several fixed concentrations of ADP (indicated above in micromolar) and varied concentrations of ATP (12.5−125 μM). The lines correspond to the best fit to eq 2, where V_{max}^{app} = 0.024 ± 0.001 μM s^{-1}, K_{mS}^{app} = 22 ± 2.5 μM, and K_{iC}^{app} = 464 ± 50 μM. (B) Mixed inhibition of ADP toward Pep-S. Initial velocity studies at 50 μM ATP in the presence of several fixed concentrations of ADP (indicated above in micromolar) and varied concentrations of Pep-S (30−90 μM). The lines correspond to the best fit to eq 4, where V_{max}^{app} = 0.10 ± 0.002 μM s^{-1}, K_{mS}^{app} = 300 ± 7 μM, K_{iC}^{app} = 4300 ± 2100 μM, and K_{iU}^{app} = 350 ± 220 μM. (C) Competitive inhibition of Pep-I toward Pep-S. Initial velocity studies at 50 μM ATP in the presence of several fixed concentrations of Pep-I (indicated above in micromolar) and varied concentrations of Pep-S (15−90 μM). The lines correspond to the best fit to eq 2 where V_{max}^{app} = 0.11 ± 0.002 μM s^{-1}, K_{mS}^{app} = 300 ± 6 μM, and K_{iC}^{app} = 294 ± 26 μM. (D) Mixed inhibition of Pep-I toward ATP. Initial velocity studies at 50 μM Pep-S in the presence of several fixed concentrations of Pep-I (indicated above in micromolar) and varied concentrations of ATP (12.5−125 μM). The lines correspond to the best fit to eq 4, where V_{max}^{app} = 0.04 ± 0.001 μM s^{-1}, K_{mS}^{app} = 26 ± 2.5 μM, K_{iC}^{app} = 455 ± 140 μM, and K_{iU}^{app} = 300 ± 110. (E) Slope replot of panel D. The line corresponds to the best fit to eq 7, where V_{max}^{app} = 0.04 ± 0.001 μM, K_{mS}^{app} = 26 ± 2.5 μM, and K_{iC}^{app} = 455 ± 140 μM.

Table 2. Inhibition Patterns for the Phosphorylation of Pep-S by eEF-2K

varied substrate	fixed substrate	inhibitor	mechanism	K_{iC}^{app} (μM)	K_{iU}^{app} (μM)
ATP[a]	Pep-S[b]	ADP[c]	competitive[d]	464 ± 50	
Pep-S[e]	ATP[f]	ADP[c]	mixed[g]	4300 ± 2100	350 ± 220
Pep-S[h]	ATP[f]	Pep-I[i]	competitive[d]	294 ± 26	
ATP[a]	Pep-S[b]	Pep-I[i]	mixed[g]	455 ± 140	300 ± 110

[a]At 12.5−125 μM. [b]At 50 μM. [c]At 0−4000 μM. [d]Best fit of the data according to eq 2 for competitive inhibition. [e]At 30−90 μM. [f]At 50 μM. [g]Best fit of the data according to eq 4 for mixed inhibition. [h]At 15−90 μM. [i]At 0−500 μM.

lines (Figure 7). In fact, the phospho-eEF2 levels in all three cell lines were increased with NH125 treatment when compared to the levels in the DMSO-treated cell lines at corresponding time points. Recently, Chen et al. also reported an induction in eEF-2 levels in a variety of cancer cell lines (H1299 non-small cell lung carcinoma, PC3 prostate cancer, HeLa cervical cancer, H460 non-small cell lung carcinoma, and C6 rat glioma) after treatment with NH125 for 6 h.[49] In our case, the phospho-eEF2 induction upon NH125 treatment was observed most severely in HEK-293T cells and to a lesser extent in MDA-MB-231 and A549 cells. In most cases, the induction of eEF2 phosphorylation was also more severe with time. HEK-293T cells showed the largest increase in the level of phospho-eEF2 over the period of 12 h. The increase in the level of eEF-2 induction was less prominent in the other two cell lines where the increase was observed only over a period of 6 h.

dx.doi.org/10.1021/bi201787p | Biochemistry 2012, 51, 2100−2112

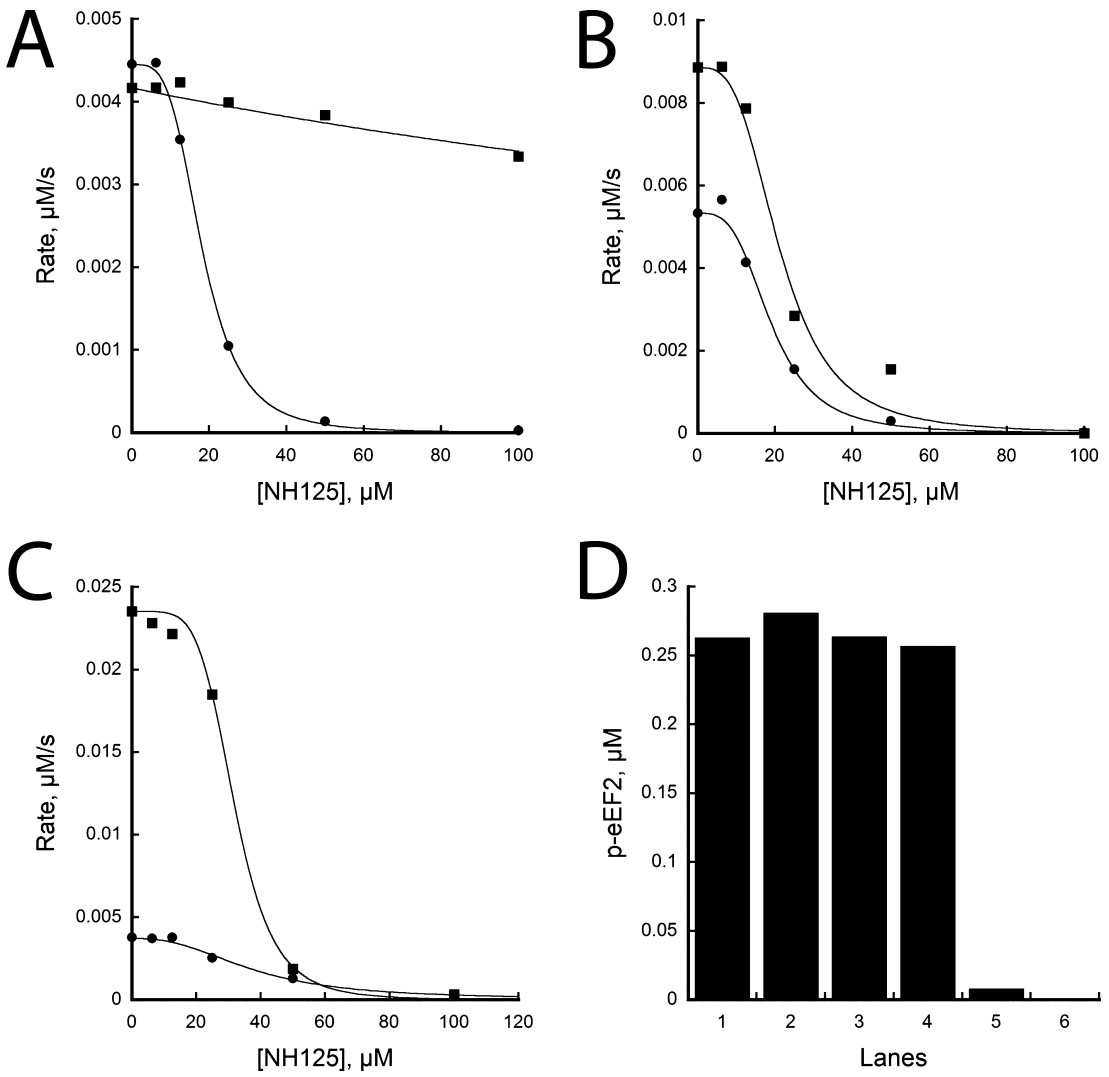

Figure 6. Inhibition of eEF-2K by NH125. (A) Dose−response curve for NH125 in the presence (■) or absence (●) of 0.1% Triton X-100. Initial rates were measured using 2 nM eEF-2K, 50 μM ATP, 30 μM Pep-S, 0 or 0.1% Triton X-100, and various concentrations of NH125 (0−100 μM). The lines correspond to the best fit to eq 8 with an IC_{50} of 18 ± 0.25 μM and a Hill coefficient of 3.7 ± 0.14. In the presence of Triton X-100, IC_{50} increases to 452 ± 243 μM with a Hill coefficient of 1.0 ± 0.28. (B) Sensitivity of the dose−response curve to ATP. Initial rates were measured using 50 (●) or 2000 μM ATP (■) in the presence of 2 nM eEF-2K, 30 μM Pep-S, and various concentrations of NH125 (0−100 μM). The lines correspond to the best fit to eq 8 with IC_{50} values of 19 ± 1.0 and 21 ± 1.6 μM in the presence of 50 and 2000 μM ATP, respectively. (C) Sensitivity of the dose−response curve to Pep-S. Initial rates were measured using 10 (●) or 100 μM Pep-S (■) in the presence of 2 nM eEF-2K, 500 μM ATP, and various concentrations of NH125 (0−100 μM). The lines correspond to the best fit to eq 8 with IC_{50} values of 37 ± 2.5 and 32 ± 5.3 μM in the presence of 10 and 100 μM Pep-S, respectively. (D) Effect of NH125 on the phosphorylation of wheat germ EF2 by eEF-2K. Phosphorylation reactions were performed in the presence of different concentrations of NH125 (0, 50, 500, and 5000 nM shown in lanes 1−4, respectively) for 10 min. Controls with no eEF-2K (lane 5) or no eEF2 (lane 6) are also shown. Phosphorylation reactions were quenched after 10 min, resolved by SDS−PAGE, and quantified using a scintillation counter.

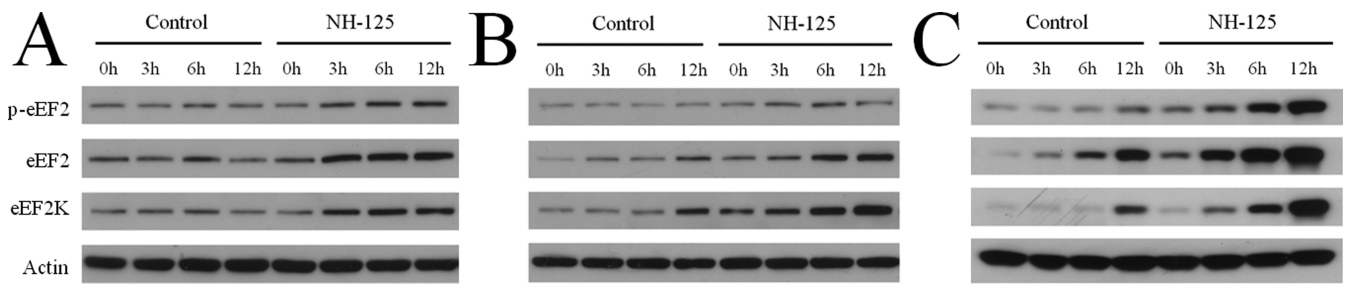

Figure 7. Cellular activity of NH125 by Western blot analysis. (A) MDA-MB-231 breast cancer, (B) A549 lung cancer, and (C) HEK-293T cells were treated with or without NH125 (4 μM) for the indicated times. The level of phosphorylation of eEF2 (Thr-56) and the levels of expression of eEF2, eEF-2K, and actin (loading control) were measured by Western blot analysis using specific antibodies (see Materials and Methods).

dx.doi.org/10.1021/bi201787p | *Biochemistry* 2012, 51, 2100−2112

In addition to the induction of phospho-eEF2, increases in the levels of eEF-2K and eEF-2 were also observed in all cell lines, which in most cases were time-dependent and correlated with the amount of phospho-eEF2 induction. Although some induction of phospho-eEF2 (in HEK-293T cells) and eEF-2K and eEF-2 (more significant in HEK-293T cells; lesser extent in A549 cells) was also observed in DMSO-treated controls, their corresponding levels were significantly higher after treatment with NH125. Taken together, these data suggest that NH125 induces eEF-2 phosphorylation through a complex process, whose robustness appears to vary depending on cell type.

DISCUSSION

Kinetic Mechanism of eEF-2K. The purpose of this study was to first assess the kinetic mechanism of recombinant human eEF-2K using a peptide substrate and then to determine its mechanism of inhibition by NH125. NH125 is a histidine kinase inhibitor that has been utilized in a number of recent studies as a specific pharmacological inhibitor of eEF-2K.[40−44] However, despite its reported potency and specificity, its mechanism of inhibition has not been determined and an activity profile against a panel of protein kinases is not available. In this study, we used a form of eEF-2K[45] that exhibits some 4000-fold higher activity toward eEF2 than a previously reported preparation.[55] Our kinetic characterization of eEF-2K with the peptide substrate unambiguously demonstrates a sequential kinetic mechanism. This is significant, because a recent structure of MHCK from *Dictyostelium* provides some support for a mechanism through a phosphoenzyme intermediate. Like eEF-2K, MHCK is an atypical protein kinase with a sequence 34% identical to that of human eEF-2K in the catalytic domain. The structure of MHCK in the presence of a peptide substrate and ATP revealed the covalent attachment of a phosphate to Asp-766, a conserved aspartate residue in the active site of MHCK, along with a bound AMP.[54] MHCK was also shown to catalyze the slow exchange of ATP and ADP at the active site. The sequential mechanism favors a direct mechanism of phosphoryl transfer between ATP and the peptide hydroxyl group, rather than a reaction through a phospho-enzyme intermediate, because the latter reaction is predicted to exhibit ping-pong kinetics. It should be noted, however, that a mechanism through a phospho-enzyme intermediate can be sequential if the release of ADP occurs after the peptide substrate binds (see, for example, Figure 2B).

Our kinetic analysis supports a mechanism of competitive substrate inhibition in which Pep-S binds eEF-2K and prevents ATP from binding. The simplest explanation for this observation is that the peptide occludes the ATP binding pocket when bound to the enzyme. Whether this is related to how the enzyme is regulated by the binding of calmodulin remains to be determined. Competitive substrate inhibition, while quite a rare mechanism for a protein kinase, is not unprecedented,[56] although the majority of protein kinases are reported to phosphorylate substrates through a random-order mechanism with little substrate inhibition (e.g., refs 57−60).

NH125 Is a Promiscuous Aggregator. NH125 was first identified as a bacterial histidine kinase inhibitor and was later reported to be a potent inhibitor of GST-eEF-2K in vitro;[40] however, the mechanism of inhibition was not determined. Recently, several laboratories have utilized NH125 to evaluate the role of eEF-2K in various biological processes. Therefore, it is essential that its mechanism be understood. We prepared an authentic sample of NH125 following a previously reported procedure[50] with some modifications (see Materials and Methods). Surprisingly, we found no evidence to suggest that NH125 exhibits potent inhibition of eEF-2K as previously reported.[40] Rather, an examination of dose−response curves of the observed rate versus the concentration of NH125 revealed an IC_{50} of 18 μM for the inhibition of peptide phosphorylation (Figure 6A). Furthermore, the dependence of the observed rate on the concentration of NH125 was best fit to a dose−response curve described by a Hill coefficient of approximately 3.7 (Figure 6A). Further analysis showed the activity of NH125 to be sensitive to added detergent (Triton X-100), an observation that further suggests that NH125 inhibits eEF-2K through aggregation. Many organic compounds form colloid-like aggregates in aqueous solution, and nonspecific inhibition of enzymes in vitro due to aggregate formation is a relatively common occurrence.[61] NH125 (Figure 1) has a structure consistent with detergent properties; i.e., it contains a polar head and long hydrophobic alkyl tail. Typically, the aggregation process is significant in the micromolar range.[62] The previous report suggested that NH125 inhibited the phosphorylation of eEF2 by GST-eEF-2K with an IC_{50} of 60 nM.[40] This observation is difficult to reconcile with the reported assay conditions where the enzyme was assayed at 400 nM, a concentration substantially above the reported IC_{50}. It is perhaps also significant that the activity of eEF-2K used to originally assess NH125 is reported to be some 10^6-fold lower than the activity of the eEF-2K used in this study (a specific activity of 1.5 pmol min^{-1} mg^{-1} was reported, which corresponds to a k_{cat} of 2.7×10^{-6} s^{-1}).[40] Taken together, our data provide strong evidence that NH125 does not inhibit eEF-2K through a conventional mechanism of inhibition but instead inhibits the enzyme through the reversible formation of a colloid.

Cellular Effect of NH125. A number of cellular studies suggest that NH125 inhibits eEF-2K activity in cells. For example, Arora et al. first reported that 1 μM NH125 strongly inhibits the phosphorylation of eEF2 in C6 glioma cells after incubation for 12 h,[40] and Khan et al. reported that a 2 h preincubation of human microvascular endothelial cells (HMVECs) with 200 nM NH125 resulted in the inhibition of resveratrol-induced eEF2 phosphorylation.[42] NH125 has also been reported to inhibit eEF-2K in vivo. For example, Autry et al. reported recently that administration of a 5 mg/kg dose of NH125 to mice for 30 min resulted in an observable decrease in the level of eEF2 phosphorylation in the hippocampus.[43] Given that NH125 inhibits eEF-2K through a nonspecific mechanism in vitro, the question of how NH125 inhibits eEF-2K both in cell lines and in vivo then arises. When we examined the ability of 4 μM NH125 to inhibit the phosphorylation of eEF2 in MDA-MB-231 breast cancer, A549 lung cancer, and HEK-293T cell lines for up to 12 h, no inhibition was observed (Figure 7). In fact, the induction of phospho-eEF2 was observed in all cell lines after treatment with NH125. Similar results were also reported in a recent study by Chen et al. using H1299 non-small cell lung carcinoma, PC3 prostate cancer, HeLa cervical cancer, H460 non-small cell lung carcinoma, and C6 rat glioma cell lines after treatment with NH125 for 6 h.[49] Although our data further indicated that the induction of eEF-2 levels by NH125 may be due to the effect of NH125 on the expression of eEF-2K and eEF-2, both our data and the reported data of Chen et al.[49] suggest that NH125 does not inhibit the phosphorylation of eEF2 and hence is not an inhibitor for eEF-2K in cells.

In summary, we have shown that eEF-2K phosphorylates a peptide substrate through a sequential mechanism. The peptide substrate inhibits the binding of ATP and must bind after ATP binds to form a productive ternary complex. The ability to evaluate potential inhibitors using the peptide substrate revealed that NH125, a frequently utilized "inhibitor" of eEF-2K,[40] does not in fact inhibit eEF-2K with high potency. In fact, it most likely inhibits eEF-2K in vitro through a nonspecific aggregation process. In addition, NH125 failed to show any inhibition of eEF-2 phosphorylation in a variety of cancer cell lines, supporting the argument that NH125 is not a cellular inhibitor of eEF-2K.

■ ASSOCIATED CONTENT

Supporting Information

Mass spectrometry and NMR data for NH125 as well as phosphorylation assays using wheat germ EF2 performed at higher concentrations of NH125. This material is available free of charge via the Internet at http://pubs.acs.org.

■ AUTHOR INFORMATION

Corresponding Author

*K.N.D.: 107 W. Dean Keaton, Biomedical Engineering Building, The University of Texas at Austin, Austin, TX 78712; e-mail, kinases@me.com; phone, (512) 471-9267; fax, (512) 232 2606. B.O.: Department of Experimental Therapeutics, Unit 422, The University of Texas M. D. Anderson Cancer Center, 1515 Holcombe Blvd., Houston, TX 77030; e-mail, bozpolat@mdanderson.org.

Funding

This research was supported in part by grants from the Welch Foundation (F-1390) to K.N.D. and the National Institutes of Health to K.N.D. (GM59802). A grant from the National Institutes of Health (P01GM078195) supported K.N.D. T.S.K. acknowledges a scholarship from the Egyptian Ministry of Higher Education.

Notes

The authors declare no competing financial interest.

■ ABBREVIATIONS

eEF-2K, elongation factor 2 kinase; eEF2, elongation factor 2; CaM, calmodulin; SAPK, stress-activated protein kinase; p90 RSK, p90 ribosomal S6 kinase; ERK, extracellular signal-regulated protein kinase; JNK, Jun N-terminal kinase; MAPK, mitogen-activated protein kinase; Rsk-2, mitogen-activated protein kinase-activated protein kinase; PKC, protein kinase C; BSA, bovine serum albumin; DTT, dithiothreitol; EDTA, ethylenediaminetetraacetic acid; EGTA, ethylene glycerol bis(2-aminoethyl ether)-*N*,*N*,*N*′,*N*′-tetraacetic acid; PMSF, phenylmethanesulfonyl fluoride; TPCK, tosylphenylalanyl-chloromethane; IPTG, isopropyl *β*-D-thiogalactopyranoside; ESI, electrospray ionization; MALDI, matrix-assisted laser desorption ionization; HPLC, high-performance liquid chromatography; Pep-S, peptide substrate (acetyl-RKKYKFNED-TERRRFL-amide); Pep-I, peptide inhibitor (acetyl-RKKYKF-NEDAERRRFL-amide).

■ REFERENCES

(1) Ryazanov, A. G. (2002) Elongation factor-2 kinase and its newly discovered relatives. *FEBS Lett. 514*, 26−29.

(2) Pavur, K. S., Petrov, A. N., and Ryazanov, A. G. (2000) Mapping the functional domains of elongation factor-2 kinase. *Biochemistry 39*, 12216−12224.

(3) Nairn, A. C., and Palfrey, H. C. (1987) Identification of the major Mr 100,000 substrate for calmodulin-dependent protein kinase III in mammalian cells as elongation factor-2. *J. Biol. Chem. 262*, 17299−17303.

(4) Ryazanov, A. G., and Spirin, A. S. (1990) Phosphorylation of elongation factor 2: A key mechanism regulating gene expression in vertebrates. *New Biol. 2*, 843−850.

(5) Redpath, N. T., Price, N. T., Severinov, K. V., and Proud, C. G. (1993) Regulation of elongation factor-2 by multisite phosphorylation. *Eur. J. Biochem. 213*, 689−699.

(6) Ryazanov, A. G., Shestakova, E. A., and Natapov, P. G. (1988) Phosphorylation of elongation factor 2 by EF-2 kinase affects rate of translation. *Nature 334*, 170−173.

(7) Carlberg, U., Nilsson, A., and Nygard, O. (1990) Functional properties of phosphorylated elongation factor 2. *Eur. J. Biochem. 191*, 639−645.

(8) Ryazanov, A. G., and Davydova, E. K. (1989) Mechanism of elongation factor 2 (EF-2) inactivation upon phosphorylation. Phosphorylated EF-2 is unable to catalyze translocation. *FEBS Lett. 251*, 187−190.

(9) Hait, W. N., Wu, H., Jin, S., and Yang, J. M. (2006) Elongation factor-2 kinase: Its role in protein synthesis and autophagy. *Autophagy 2*, 294−296.

(10) Wu, H., Yang, J. M., Jin, S., Zhang, H., and Hait, W. N. (2006) Elongation factor-2 kinase regulates autophagy in human glioblastoma cells. *Cancer Res. 66*, 3015−3023.

(11) Meijer, A. J., and Codogno, P. (2004) Regulation and role of autophagy in mammalian cells. *Int. J. Biochem. Cell Biol. 36*, 2445−2462.

(12) Levine, B., and Kroemer, G. (2008) Autophagy in the pathogenesis of disease. *Cell 132*, 27−42.

(13) Bursch, W., Ellinger, A., Kienzl, H., Torok, L., Pandey, S., Sikorska, M., Walker, R., and Hermann, R. S. (1996) Active cell death induced by the anti-estrogens tamoxifen and ICI 164 384 in human mammary carcinoma cells (MCF-7) in culture: The role of autophagy. *Carcinogenesis 17*, 1595−1607.

(14) Bursch, W., Hochegger, K., Torok, L., Marian, B., Ellinger, A., and Hermann, R. S. (2000) Autophagic and apoptotic types of programmed cell death exhibit different fates of cytoskeletal filaments. *J. Cell Sci. 113* (Part 7), 1189−1198.

(15) Scarlatti, F., Bauvy, C., Ventruti, A., Sala, G., Cluzeaud, F., Vandewalle, A., Ghidoni, R., and Codogno, P. (2004) Ceramide-mediated macroautophagy involves inhibition of protein kinase B and up-regulation of beclin 1. *J. Biol. Chem. 279*, 18384−18391.

(16) Paglin, S., Hollister, T., Delohery, T., Hackett, N., McMahill, M., Sphicas, E., Domingo, D., and Yahalom, J. (2001) A novel response of cancer cells to radiation involves autophagy and formation of acidic vesicles. *Cancer Res. 61*, 439−444.

(17) Yao, K. C., Komata, T., Kondo, Y., Kanzawa, T., Kondo, S., and Germano, I. M. (2003) Molecular response of human glioblastoma multiforme cells to ionizing radiation: Cell cycle arrest, modulation of the expression of cyclin-dependent kinase inhibitors, and autophagy. *J. Neurosurg. 98*, 378−384.

(18) Ito, H., Daido, S., Kanzawa, T., Kondo, S., and Kondo, Y. (2005) Radiation-induced autophagy is associated with LC3 and its inhibition sensitizes malignant glioma cells. *Int. J. Oncol. 26*, 1401−1410.

(19) Kanzawa, T., Kondo, Y., Ito, H., Kondo, S., and Germano, I. (2003) Induction of autophagic cell death in malignant glioma cells by arsenic trioxide. *Cancer Res. 63*, 2103−2108.

(20) Takeuchi, H., Kondo, Y., Fujiwara, K., Kanzawa, T., Aoki, H., Mills, G. B., and Kondo, S. (2005) Synergistic augmentation of rapamycin-induced autophagy in malignant glioma cells by phosphatidylinositol 3-kinase/protein kinase B inhibitors. *Cancer Res. 65*, 3336−3346.

(21) Kanzawa, T., Germano, I. M., Komata, T., Ito, H., Kondo, Y., and Kondo, S. (2004) Role of autophagy in Temozolomide-induced cytotoxicity for malignant glioma cells. *Cell Death Differ. 11*, 448−457.
(22) Opipari, A. W. Jr., Tan, L., Boitano, A. E., Sorenson, D. R., Aurora, A., and Liu, J. R. (2004) Resveratrol-induced autophagocytosis in ovarian cancer cells. *Cancer Res. 64*, 696−703.
(23) Ellington, A. A., Berhow, M., and Singletary, K. W. (2005) Induction of macroautophagy in human colon cancer cells by soybean B-group triterpenoid saponins. *Carcinogenesis 26*, 159−167.
(24) Ellington, A. A., Berhow, M. A., and Singletary, K. W. (2006) Inhibition of Akt signaling and enhanced ERK1/2 activity are involved in induction of macroautophagy by triterpenoid B-group soyasaponins in colon cancer cells. *Carcinogenesis 27*, 298−306.
(25) Hoyer-Hansen, M., Bastholm, L., Mathiasen, I. S., Elling, F., and Jaattela, M. (2005) Vitamin D analog EB1089 triggers dramatic lysosomal changes and Beclin 1-mediated autophagic cell death. *Cell Death Differ. 12*, 1297−1309.
(26) Shao, Y., Gao, Z., Marks, P. A., and Jiang, X. (2004) Apoptotic and autophagic cell death induced by histone deacetylase inhibitors. *Proc. Natl. Acad. Sci. U.S.A. 101*, 18030−18035.
(27) Kondo, Y., and Kondo, S. (2006) Autophagy and cancer therapy. *Autophagy 2*, 85−90.
(28) Kondo, Y., Kanzawa, T., Sawaya, R., and Kondo, S. (2005) The role of autophagy in cancer development and response to therapy. *Nat. Rev. Cancer 5*, 726−734.
(29) Wu, H., Zhu, H., Liu, D. X., Niu, T. K., Ren, X., Patel, R., Hait, W. N., and Yang, J. M. (2009) Silencing of elongation factor-2 kinase potentiates the effect of 2-deoxy-D-glucose against human glioma cells through blunting of autophagy. *Cancer Res. 69*, 2453−2460.
(30) Calberg, U., Nilsson, A., Skog, S., Palmquist, K., and Nygard, O. (1991) Increased activity of the eEF-2 specific, Ca^{2+} and calmodulin dependent protein kinase III during the S-phase in Ehrlich ascites cells. *Biochem. Biophys. Res. Commun. 180*, 1372−1376.
(31) Parmer, T. G., Ward, M. D., Yurkow, E. J., Vyas, V. H., Kearney, T. J., and Hait, W. N. (1999) Activity and regulation by growth factors of calmodulin-dependent protein kinase III (elongation factor 2-kinase) in human breast cancer. *Br. J. Cancer 79*, 59−64.
(32) Bagaglio, D. M., Cheng, E. H., Gorelick, F. S., Mitsui, K., Nairn, A. C., and Hait, W. N. (1993) Phosphorylation of elongation factor 2 in normal and malignant rat glial cells. *Cancer Res. 53*, 2260−2264.
(33) Hait, W. N., Ward, M. D., Trakht, I. N., and Ryazanov, A. G. (1996) Elongation factor-2 kinase: Immunological evidence for the existence of tissue-specific isoforms. *FEBS Lett. 397*, 55−60.
(34) Parmer, T. G., Ward, M. D., and Hait, W. N. (1997) Effects of rottlerin, an inhibitor of calmodulin-dependent protein kinase III, on cellular proliferation, viability, and cell cycle distribution in malignant glioma cells. *Cell Growth Differ. 8*, 327−334.
(35) Bagaglio, D. M., and Hait, W. N. (1994) Role of calmodulin-dependent phosphorylation of elongation factor 2 in the proliferation of rat glial cells. *Cell Growth Differ. 5*, 1403−1408.
(36) Smith, E. M., and Proud, C. G. (2008) cdc2-cyclin B regulates eEF2 kinase activity in a cell cycle- and amino acid-dependent manner. *EMBO J. 27*, 1005−1016.
(37) Cho, S. I., Koketsu, M., Ishihara, H., Matsushita, M., Nairn, A. C., Fukazawa, H., and Uehara, Y. (2000) Novel compounds, '1,3-selenazine derivatives' as specific inhibitors of eukaryotic elongation factor-2 kinase. *Biochim. Biophys. Acta 1475*, 207−215.
(38) Gschwendt, M., Kittstein, W., and Marks, F. (1994) Elongation factor-2 kinase: Effective inhibition by the novel protein kinase inhibitor rottlerin and relative insensitivity towards staurosporine. *FEBS Lett. 338*, 85−88.
(39) Lockman, J. W., Reeder, M. D., Suzuki, K., Ostanin, K., Hoff, R., Bhoite, L., Austin, H., Baichwal, V., and Adam Willardsen, J. (2010) Inhibition of eEF2-K by thieno[2,3-b]pyridine analogues. *Bioorg. Med. Chem. Lett. 20*, 2283−2286.
(40) Arora, S., Yang, J. M., Kinzy, T. G., Utsumi, R., Okamoto, T., Kitayama, T., Ortiz, P. A., and Hait, W. N. (2003) Identification and characterization of an inhibitor of eukaryotic elongation factor 2 kinase against human cancer cell lines. *Cancer Res. 63*, 6894−6899.
(41) Rose, A. J., Alsted, T. J., Jensen, T. E., Kobbero, J. B., Maarbjerg, S. J., Jensen, J., and Richter, E. A. (2009) A Ca^{2+}-calmodulin-eEF2K-eEF2 signalling cascade, but not AMPK, contributes to the suppression of skeletal muscle protein synthesis during contractions. *J. Physiol. 587*, 1547−1563.
(42) Khan, A. A., Dace, D. S., Ryazanov, A. G., Kelly, J., and Apte, R. S. (2010) Resveratrol regulates pathologic angiogenesis by a eukaryotic elongation factor-2 kinase-regulated pathway. *Am. J. Pathol. 177*, 481−492.
(43) Autry, A. E., Adachi, M., Nosyreva, E., Na, E. S., Los, M. F., Cheng, P. F., Kavalali, E. T., and Monteggia, L. M. (2011) NMDA receptor blockade at rest triggers rapid behavioural antidepressant responses. *Nature 475*, 91−95.
(44) Belle, R., Pluchon, P. F., Cormier, P., and Mulner-Lorillon, O. (2011) Identification of a new isoform of eEF2 whose phosphorylation is required for completion of cell division in sea urchin embryos. *Dev. Biol. 350*, 476−483.
(45) Abramczyk, O., Tavares, C. D., Devkota, A. K., Ryazanov, A. G., Turk, B. E., Riggs, A. F., Ozpolat, B., and Dalby, K. N. (2011) Purification and characterization of tagless recombinant human elongation factor 2 kinase (eEF-2K) expressed in *Escherichia coli*. *Protein Expression Purif. 79*, 237−244.
(46) McGovern, S. L., Helfand, B. T., Feng, B., and Shoichet, B. K. (2003) A specific mechanism of nonspecific inhibition. *J. Med. Chem. 46*, 4265−4272.
(47) Feng, B. Y., and Shoichet, B. K. (2006) A detergent-based assay for the detection of promiscuous inhibitors. *Nat. Protoc. 1*, 550−553.
(48) Ryan, A. J., Gray, N. M., Lowe, P. N., and Chung, C. W. (2003) Effect of detergent on "promiscuous" inhibitors. *J. Med. Chem. 46*, 3448−3451.
(49) Chen, Z., Gopalakrishnan, S. M., Bui, M. H., Soni, N. B., Warrior, U., Johnson, E. F., Donnelly, J. B., and Glaser, K. B. (2011) 1-Benzyl-3-cetyl-2-methylimidazolium iodide (NH125) induces phosphorylation of eukaryotic elongation factor-2 (eEF2): A cautionary note on the anticancer mechanism of an eEF2 kinase inhibitor. *J. Biol. Chem. 286*, 43951−43958.
(50) Yamamoto, K., Kitayama, T., Ishida, N., Watanabe, T., Tanabe, H., Takatani, M., Okamoto, T., and Utsumi, R. (2000) Identification and characterization of a potent antibacterial agent, NH125 against drug-resistant bacteria. *Biosci., Biotechnol., Biochem. 64*, 919−923.
(51) Smailov, S. K., Lee, A. V., and Iskakov, B. K. (1993) Study of phosphorylation of translation elongation factor 2 (EF-2) from wheat germ. *FEBS Lett. 321*, 219−223.
(52) Segel, I. H. (1993) *Enzyme Kinetics: Behaviour and analysis of Rapid Equilibrium and Steady-State Enzyme Systems*, Wiley Classics Library Edition, John Wiley & Sons, Inc., New York.
(53) Copeland, R. A. (2005) Evaluation of enzyme inhibitors in drug discovery. A guide for medicinal chemists and pharmacologists. *Methods Biochem. Anal. 46*, 1−265.
(54) Ye, Q., Crawley, S. W., Yang, Y., Cote, G. P., and Jia, Z. (2010) Crystal structure of the α-kinase domain of *Dictyostelium* myosin heavy chain kinase A. *Sci. Signaling 3*, ra17.
(55) Crawley, S. W., and Cote, G. P. (2008) Determinants for substrate phosphorylation by *Dictyostelium* myosin II heavy chain kinases A and B and eukaryotic elongation factor-2 kinase. *Biochim. Biophys. Acta 1784*, 908−915.
(56) Keshwani, M. M., Gao, X., and Harris, T. K. (2009) Mechanism of PDK1-catalyzed Thr-229 phosphorylation of the S6K1 protein kinase. *J. Biol. Chem. 284*, 22611−22624.
(57) Cook, P. F., Neville, M. E. Jr., Vrana, K. E., Hartl, F. T., and Roskoski, R. Jr. (1982) Adenosine cyclic 3′,5′-monophosphate dependent protein kinase: Kinetic mechanism for the bovine skeletal muscle catalytic subunit. *Biochemistry 21*, 5794−5799.
(58) Kong, C. T., and Cook, P. F. (1988) Isotope partitioning in the adenosine 3′,5′-monophosphate dependent protein kinase reaction indicates a steady-state random kinetic mechanism. *Biochemistry 27*, 4795−4799.

(59) Waas, W. F., and Dalby, K. N. (2003) Physiological concentrations of divalent magnesium ion activate the serine/threonine specific protein kinase ERK2. *Biochemistry 42*, 2960−2970.
(60) Niu, L., Chang, K. C., Wilson, S., Tran, P., Zuo, F., and Swinney, D. C. (2007) Kinetic characterization of human JNK2α2 reaction mechanism using substrate competitive inhibitors. *Biochemistry 46*, 4775−4784.
(61) Seidler, J., McGovern, S. L., Doman, T. N., and Shoichet, B. K. (2003) Identification and prediction of promiscuous aggregating inhibitors among known drugs. *J. Med. Chem. 46*, 4477−4486.
(62) McGovern, S. L., and Shoichet, B. K. (2003) Kinase inhibitors: Not just for kinases anymore. *J. Med. Chem. 46*, 1478−1483.
(63) Soltoff, S. P. (2007) Rottlerin: An inappropriate and ineffective inhibitor of PKCδ. *Trends Pharmacol. Sci. 28*, 453−458.
(64) Soltoff, S. P. (2001) Rottlerin is a mitochondrial uncoupler that decreases cellular ATP levels and indirectly blocks protein kinase Cδ tyrosine phosphorylation. *J. Biol. Chem. 276*, 37986−37992.
(65) Yamamoto, K., Kitayama, T., Minagawa, S., Watanabe, T., Sawada, S., Okamoto, T., and Utsumi, R. (2001) Antibacterial agents that inhibit histidine protein kinase YycG of *Bacillus subtilis*. *Biosci., Biotechnol., Biochem. 65*, 2306−2310.
(66) Tavares, C. D. J., O'Brien, J. P., Abramczyk, O., Devkota, A. K., Shores, K. S., Ferguson, S. B., Kaoud, T. S., Warthaka, M., Marshall, K. D., Keller, K. M., Zhang, Y., Brodbelt, J. S., Ozpolat, B., and Dalby, K. N. (2012) Calcium/calmodulin stimulates the autophosphorylation of elongation factor 2 kinase on Thr-348 and Ser-500 to regulate its activity and calcium dependence. *Biochemistry*, DOI: 10.1021/bi201788e.